JHMI
Journal of Health Management and Informatics

Original Article

Sparse Representation-Based Classification (SRC): A Novel Method to Improve the Performance of Convolutional Neural Networks in Detecting P300 Signals

Seyed Vahab Shojaedini*, Sajedeh Morabbi

Department of Biomedical Engineering, Iranian Research Organization for Science and Technology, Tehran, Iran

Abstract

Introduction: Brain-Computer Interface (BCI) offers a non-muscle way between the human brain and the outside world to make a better life for disabled people. In BCI applications P300 signal has an effective role; therefore, distinguishing P300 and non-P300 components in EEG signal (i.e. P300 detection) becomes a vital problem in BCI applications. Recently, Convolutional Neural Networks (CNNs) have had a significant application in detection of P300 signals in the field of BCIs. The P300 signal has low Signal to Noise Ratio (SNR). On the other hand, the CNN detection rate is so sensitive to SNR; therefore, CNN detection rate drops dramatically when it is faces with P300 data. In this study, a novel structure is proposed to improve the performance of CNN in P300 signal detection by means of improving its performance against low SNR signals.

Methods: In the proposed structure, Sparse Representation-based Classification (SRC) was used as the first substructure. This block is responsible for prediction of the expected P300 signal among artifacts and noise. The second substructure performed P300 classification with Adadelta algorithm. Thanks to such SNR improvement scheme; the proposed structure is able to increase the rate of accuracy in the field of P300 signal detection.

Results: To evaluate the performance of the proposed structure, we applied it on EPFL dataset for P300 detection, and then the achieved results were compared with those obtained from the basic CNN structure. The comparisons revealed the superiority of the proposed structure against its alternative, so that its True Positive Rate (TPR) was promoted about 19.66%. Such improvements for false detections and accuracy parameters were 1.93% and 10.46%, respectively, which show the effectiveness of applying the proposed structure in detecting P300 signals.

Conclusion: The better accuracy of the proposed algorithm compared to basic CNN, in parallel with its more robustness, showed that the Sparse Representation-based Classification (SRC) had a considerable potential to be used as an improving idea in CNN-based P300 detection.

Keywords: EEG, Neural Networks, Signal Detection, Machine Learning, Brain-Computer Interfaces, Brain-Computer Interface, Brain, Neuroscience, P300, Convolutional Neural Networks, Deep Learning

*Correspondence to:
Seyed Vahab Shojaedini
Department of Biomedical Engineering, Iranian Research Organization for Science and Technology, Tehran, Iran
Tel: +98-21-56276311
Fax: +98-21-56276620
Email: shojadini@irost.ir

Introduction

Brain Computer Interface (BCI) is a communication system that allows the brain to control devices without any peripheral muscle activity (1, 2). The BCIs have been traditionally developed to assist people who are unable to move despite retaining their cognitive abilities; also, they are used to improve the quality of life and reduce the social costs (1, 3)

Event Related Potentials (ERPs) are evoked brain responses synchronized to sensory, cognitive and motor events which are widely used in BCI applications. Therefore, they consist of relatively reproducible wave shapes embedded in the background of Electroencephalogram (EEG) activity. Generally, P300 signal has a positive peak that is evoked almost 300 *ms* after the first stimulus (4, 5).

An oddball paradigm is a common way to excite the subjects under test for obtaining their P300 signals. It is a square matrix containing alphabetic, numeric and under line symbols. These symbols are randomly intensified in a special row and column of certain and predefined word's characters which were displayed continually to the subjects for evoked P300 potential (6).

Unfortunately, the P300 signal has low Signal to

Noise Ratio (SNR) which hampers its application in many of BCI systems. For several years, averaging has been used to improve the SNR, but this method has deformed the P300 signal because of the decrease in its bit rate (4, 7). Nowadays, artificial intelligence techniques have been applied to increase the SNR without loss of any significant information of the P300 signal (8).

Artificial intelligence methods in the field of P300 signal detection include linear and nonlinear methods (4, 8). The linear techniques have simple structures to understand and use, but they are not strong enough to deal with real-complex problems. On the other hand, the non-linear techniques are powerful to face with complex problems in the real world, but their main weakness is over-fitting (9).

In recent years, neural networks have had a wide development in the BCI applications also in the field of P300 detection (10). The main drawback of this approach is the need to additional preprocessing step as feature extraction because neural networks mainly require appropriate features as its input data (11). To address this problem, numerous researchers have been applied in field of Deep Neural Networks (DNN) for P300 signal detection (2). DNNs are a typical type of neural networks which use the signal directly as their input data to extract the features automatically (11). Moreover, they have a deep dimension with multilevel representation of data (12), which enables the model to express more complicated neurobiological problems.

Convolutional Neural Network (CNN) is a class of DDNs which has been widely used in P300 signal detection and classification (13, 14). In some applications, CNN was used in order to enhance the performance of P300 classification and detection and preserve spatio-temporal features of the EEG signal (12, 15). Unfortunately, the CNN detection rate drops dramatically when they are faced with noise and artifact in the input data (16). In this study, a new structure is introduced to improve the detection rate of the P300 signal among additional noise (i.e. artifacts) by using CNN. The proposed structure includes two substructures; the first one is responsible for predicting the expected P300 signal among the artifacts and the second substructure performs P300 classification with Adadelta algorithm. The aim of the proposed structure is to improve the SNR in BCIs, so it is able to increase the rate of accuracy in the field of P300 signal detection.

In the next part the principles of the proposed method are described, the real data is tested, and finally the results obtained from the proposed method and its alternative schemes are compared.

Methods

The EEG data of the EPFL dataset include eight normal and disabled subjects. The data were obtained using Biosemi system with 32 channels in 2048 HZ. The electrodes were located based on 10-20 system positioning standard. The EEG data of each subject consisted of four sessions and the data of each session was composed of six runs which corresponded to six images. The images were displayed in the laptop screen to evoke the related potential and they were based on random order for 100 ms; during 300 ms, none of them was depicted. More details about the EPFL dataset can be found in (17).

In machine learning, a CNN is a type of deep, feed forward artificial neural networks which use a variety of multilayer perceptrons designed to require minimal preprocessing (18). This type of neural networks is also known as shift invariant or space invariant artificial neural network (SIANN), based on their shared-weights architecture and translation invariance characteristics (19, 20).

CNNs were inspired by biological processes (21) in that the connectivity pattern between the neurons resembles the organization of the animal visual cortex.

The receptive field of an individual sensory neuron is the particular region of the sensory space (e.g. the body surface, or the visual field) in which a stimulus will modify the firing of that neuron. . The main CNN layers which make its body are: convolutional layer, pooling layer and fully connected layer.

The convolutional layer is the core building block of a CNN that does most of the computational heavy lifting. The convolutional layer's parameters consist of a set of learnable filters. Every filter is small spatially (along width and height), but it extends through the full depth of the input volume. .During the forward pass, each filter slips across the input volume and dot products are computed between the entries of the filter and the input.

As the filter slides over the width and height of the input volume, an activation map that gives the responses of that filter at every spatial position is produced (22).

In general, the task of the pooling layer is to progressively reduce the spatial size of the representation, in order to reduce the computational cost in the network which leads to control of the over-fitting. . There are two types of pooling, average and max. In practice, the max pooling led to better convergence during training process. The neurons

in a fully connected layer have full connections to all activations in the previous layer, as seen in regular neural networks. Their activations may, hence, be computed with a matrix multiplication followed by a bias offset (22).

Sparse Representation-based Classification

The EEG signal is often captured with low SNR which is challenging in neurology problems. Hence, the P300 signal detection problem still faces an important issue regarding the low SNR. In practice, when the input data of CNN is mixed with artifacts, its recognition rate is dramatically reduced. To address this problem, a novel method based on Sparse Representation-based Classification (SRC) is proposed as a SNR improving approach which extracts the features which are independent from noise and improve the P300 signal detection.

In SRC, the training set may be supposed as a dictionary, $dic=[dic_{P300}, dic_{nonP300}]$, where dic_{P300} and $dicnon_{P300}$ are sub-dictionaries which correspond to P300 and non-P300 signals in the training set. A new signal sample with low SNR $\tilde{s}$ may be defined with a linear combination of some columns in dic as (23):

$$\tilde{s} = [dic_{P300}, dic_{nonP300}] \begin{bmatrix} c_{P300} \\ c_{nonP300} \end{bmatrix} \tag{1}$$

Where the coefficient vectors $[C_{P300} \quad C_{nonP300}]$ are faced with sparsity by different sparsity constraints. The identity of $\tilde{s}$ may be rewrite as below (24):

$$iden(\tilde{s}) = \arg min_{j \in \{P300, nonP300\}} \left\| \tilde{s} - dic_j.c_j \right\|_2 \tag{2}$$

In equation (2), $\arg min_{j \in \{P300, nonP300\}} \left\| \tilde{s} - dic_j.c_j \right\|_2$ find the class which contributes more to the reconstruction of the input signal $\tilde{s}$.

A new sample may be generated using randomly selecting a signal sample from $[dic_{P300}, dic_{nonP300}]$, as s and additional noise as n:

$$\tilde{s} = s + n \tag{3}$$

In Figure 1, the input of the proposed structure is $S+n$ which refers to a combination of s as the expected signal captured at ideal condition and n is a representation of the artifact or noise.

The first part of the proposed structure is a substructure aiming to learn a mapping function $F(\tilde{s}) = s$ to predict the expected signal s from noisy signal $\tilde{s}$. Moreover, the averaged mean squared error between these signals is forced to be small, which is defined as the following equation:

$$\arg min \frac{1}{2M} \sum_{j=1}^{M} \left\| \tilde{s}_j - s_j \right\|_2^2 = \frac{1}{2M} \left\| \tilde{S} - S \right\|_\rho^2 \tag{4}$$

Where M is the total number of training signals,

$S = [s_1, \cdots, s_M]$ and $\tilde{S} = [\tilde{s}_1, \cdots, \tilde{s}_M]$. Then, the predicted expected signal s is fed to the first convolutional layer as the first layer of the second sub-structure. Discrete convolution between signal s and the filter $Filt$ is computed as (25):

$$\theta = \sum_{q=1}^{M} Filt_q.s_q \tag{5}$$

Where θ refers to model weights.

Optimizer Algorithm

Here, Adadelta is used as training algorithm. It restricts the window of accumulated past gradients to some fixed size w, instead of inefficiently storing w previous squared gradients. The sum of gradients is recursively defined as a decaying average of all the previously squared gradients. The running average $E[g^2]_t$ at time step t then depends (as a fraction γ similarly on the momentum term and g is the gradient of θ) only on the previous average and the current gradient (26):

$$E[g^2]_t = \gamma E[g^2]_{t-1} + (1-\gamma)g_t^2 \tag{6}$$

To rewrite the Adadelta update, we used the parameter update vector $\Delta\theta_t$ in equations (7), in which α is the learning rate:

$$\Delta\theta_t = -\alpha g_{t,i}$$
$$\theta_{t+1} = \theta_t + \Delta\theta_t \tag{7}$$

The parameter update vector of Adagrad takes the form:

$$\Delta\theta_t = -\frac{\alpha}{\sqrt{G_t + \epsilon}} \odot g_t \tag{8}$$

Where, ϵ is the value that prevents the division error from zero, and G_t refers to the sum of the squares of previous gradients. Now, simply the diagonal matrix G_t is replaced with the decaying average over the previously squared gradients $E[g^2]_t$, as described in equation (9):

$$\Delta\theta_t = -\frac{\alpha}{\sqrt{E[g^2]_t + \epsilon}} g_t \tag{9}$$

As the denominator is just the root mean squared (RMS) error criterion of the gradient, a short hand form is replaced with it:
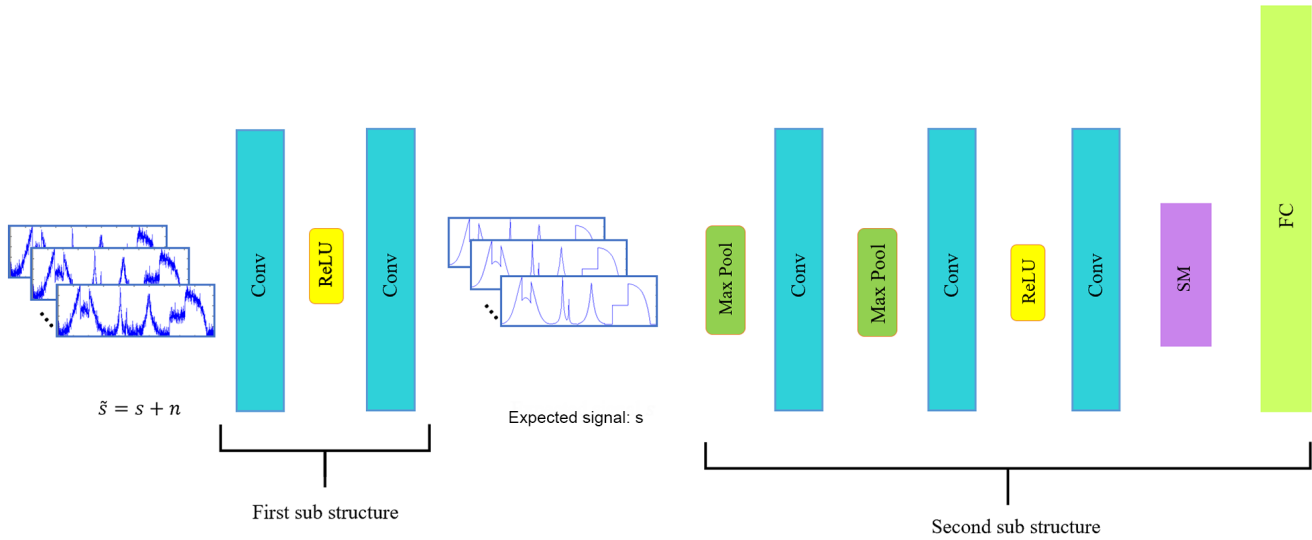
$$\Delta\theta_t = -\frac{\alpha}{RMS[g]_t} g_t \tag{10}$$

So, the equation (6) may be rewritten as follows (26):

$$E[\Delta\theta^2]_t = \gamma E[\Delta\theta^2]_{t-1} + (1-\gamma)\Delta\theta^2 \tag{11}$$

The root mean squared error of parameter updates is thus:

$$RMS[\Delta\theta]_t = \sqrt{E[\Delta\theta^2]_t + \epsilon} \tag{12}$$

Figure 1: The proposed structure for P300 signal detection which is composed of two sub structures. The first structure is responsible for predicting the expected signal and the second structure does the classification of the predicted signal into two class P300 and non-P300.

Since $RMS[\Delta\theta]_t$ is unknown, it is approximated with the RMS of parameter updates until the previous time step. Replacing the learning rate α in the previous update rule with $RMS[\Delta\theta]_{t-1}$ finally yields the following equation:

$$\Delta\theta_t = -\frac{RMS[\Delta\theta]_{t-1}}{RMS[g]_t}\, g_t$$

$$\theta_{t+1} = \theta_t + \Delta\theta_t$$

(13)

As illustrated in Figure 1, in the proposed structure, corrupted P300 signals (i.e. with artifact) are given as input; then, the first sub-structure predicts the expected version of signal. The first part of the proposed structure is composed of two convolutional layers and one Rectified Linear Unit (ReLU) as activation function between them. The output of this sub- structure is fed to the next sub-structure to be classified. The second structure is composed of three convolutional layers, two max pooling layers, one ReLU, one SoftMax (SM) layer and finally Fully Connected (FC) layer which is responsible for

computing the score of each class and putting the signal in the class with high score. Further details about the specification of the proposed structure can be found in Table 1.

Results

As described in section 2 the proposed structure was applied on EPFL dataset which had been captured from eight available subjects using 32 electrodes. It was implemented by MATLAB R2017a, on a laptop with an Intel Core i7 processor and 2 TB RAM. Four sessions are the whole-body data of each subject in the EPFL dataset. In each session, there are six runs and each run corresponds to each of the six images, which are displayed for subjects to stimulate the P300 signal.

To measure the performance of the proposed structure, we used the data of the two sessions as the training set. The data of another session are used for validation; thus, the data of leave off session was used as the test set. Four-fold-cross-validation

Table 1: The spacification of the proposed structure

Layer	Kernel	Stride	Pad	Neuron
Convolution	5x5	1	1	20
ReLU	-	-	-	-
Convolution	5x5	1	1	20
Max Pooling	2x2	2	0	20
Convolution	5x5	1	0	50
Max Pooling	2x2	2	0	50
Convolution	4x4	1	0	500
ReLU	-	-	-	-
Convolution	2x2	1	0	2

method was used to evaluate how good the proposed structure works against its alternatives (i.e. basic structure which is trained using Adadelta, Adam and RMSprop). This process was repeated four times, so each session was presented once for test. Finally, the averaged values of the results were estimated based on evaluation parameters.

The evaluation parameters consisted of True Positive Rate (TPR), True Negative Rate (TNR), False Positive Rate (FPR), False Negative Rate (FNR), classification accuracy and recall (2), which were employed to estimate the performance of the proposed structure and its state-of-the-art alternatives. As shown in Table 2, the proposed structure outperformed all of the examined parameters in all subjects, against its alternatives as described below:

The obtained TPRs revealed that the best value gained by using the proposed structure has been equal to 98.51% in subject 6, while the best TPRs obtained by applying the alternatives (i.e. basic structure which is trained using Adadelta, Adam and RMSprop algorithms) over EPFL dataset were equal to 78.85%, 83.19% and 80.55% over subject 7, respectively.

According to FPRs and FNRs, the proposed structure achieved the best values equal to 0.21% (in subjects 2 and 7 for FPR) and 1.48% (in subject 6 for FNR). The best obtained FPRs for alternatives were equal to 2.14%, 2.58% and 2.31%, respectively. Moreover, the best FNRs of the alternatives were equal to 21.1%, 16.8% and 19.44%, respectively.

Exploring the TNRs showed that the best value obtained by the proposed structure (i.e. 99.78% in subjects 2 and 7) was better than all the alternatives (i.e. 97.85% in subject 3 for basic structure trained with Adadelta, 97.41% in subject 4 for basic structure trained with Adam, and 97.68% in subject 2 for basic structure trained with RMSprop).

Similarly, the recalls showed that the best value

Table 2: The average of evaluation parameters in each subject

Type	Subject	TPR	FPR	TNR	FNR	Recall	Accuracy
Basic Structure Trained on Adadelta	1	70.74	8.86	91.13	29.25	70.74	80.93
	2	67.45	5.35	94.64	32.54	67.45	81.05
	3	77.18	2.14	97.85	22.81	77.18	87.51
	4	68.39	3.24	96.75	31.60	68.39	82.57
	5	76	5.14	94.85	23.99	76	83.41
	6	72.61	3.22	96.77	27.38	72.61	84.69
	7	78.85	2.23	97.77	21.14	78.85	88.31
	8	61.79	2.75	97.24	38.20	61.79	79.52
Basic Structure Trained on Adam	1	63.67	3.28	96.71	36.32	63.67	80.19
	2	65.84	4.93	95.06	34.15	65.84	80.45
	3	73.51	5.15	94.84	26.48	73.51	84.18
	4	72.31	2.58	97.41	27.68	72.31	84.86
	5	70.96	6.87	93.12	29.03	70.96	82.04
	6	72.11	3.51	96.48	27.88	72.11	84.30
	7	83.19	3.96	96.03	16.80	83.19	89.61
	8	75.42	17.06	82.93	24.57	75.42	79.17
Basic Structure Trained on RMSprop	1	57.80	2.72	97.27	42.19	57.8	77.53
	2	55.59	2.31	97.68	44.40	55.59	76.64
	3	79.19	5.93	94.06	20.80	79.19	86.62
	4	72.38	2.90	97.09	27.61	72.38	84.74
	5	70.28	6.22	93.77	29.71	70.28	82.02
	6	75.64	3.03	96.96	24.35	75.64	86.30
	7	80.55	2.98	97.01	19.44	80.55	88.78
	8	63.03	4.29	95.70	36.96	63.03	79.36
Proposed Structure	1	92.40	1.87	98.12	7.59	92.4	95.26
	2	95.12	0.21	99.78	4.88	95.12	97.45
	3	91.42	2.76	97.23	8.58	91.42	94.32
	4	97.55	0.40	99.59	2.44	97.55	98.57
	5	85.66	2.47	97.52	14.34	85.66	91.59
	6	98.51	0.51	99.42	1.48	98.51	98.97
	7	97.75	0.21	99.78	2.24	97.75	98.77
	8	93.29	2.29	97.74	6.70	93.29	95.51

of the proposed structure occurred in subject 6 which was 98.51%; this result shows the superiority of the proposed structure against the best results of its alternatives (i.e. 78.85% in subject 7 for basic structure trained with Adadelta, 83.19% in subject 7 for basic structure trained with Adam, and 80.55% in subject 7 for basic structure trained with RMSprop).
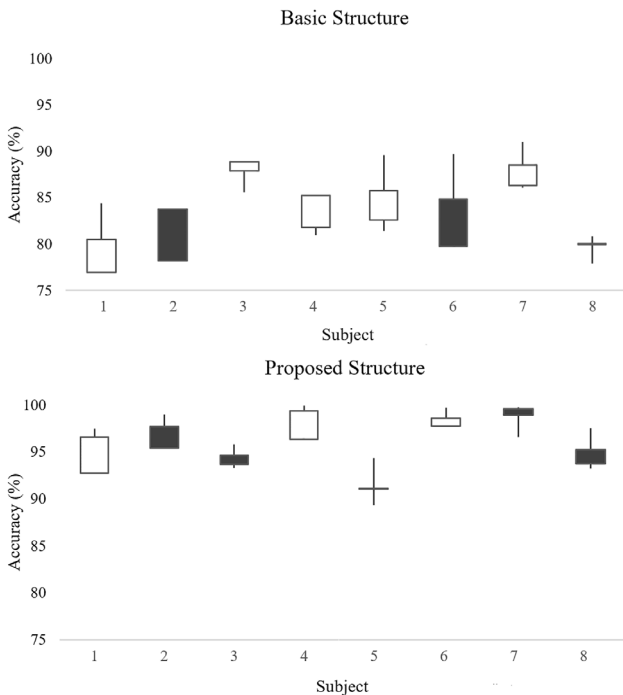
Eventually, the best classification accuracy of the proposed structure confirmed its better performance (i.e. 98.97% in subject 7) against the alternatives (i.e. 88.31% for basic structure trained by Adadelta, 89.61% for basic structure trained by Adam, and 88.78% for basic structure trained by RMSprop, all the values were obtained in subject 7).

The EPFL dataset contains EEG raw data for eight available subjects. Each subject was composed of four sessions. Therefore, the four-fold-cross-validation method was applied to use each of four data sessions in test. As depicted in Figures 2, 3 and 4, the averaged data of each subject were evaluated over all of the four sessions. Hence, the results describe how good each subject has recognized the P300 signal over all sessions based on the examined parameters (i.e. accuracy, TPR and FP
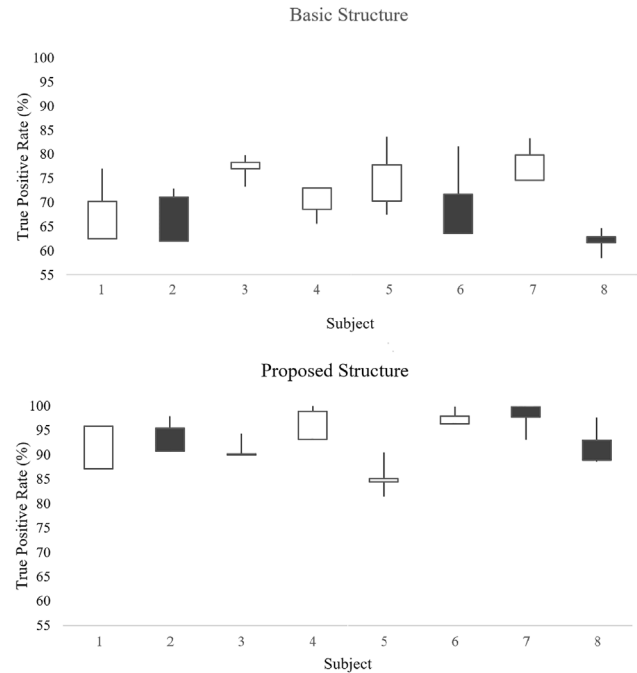
Among alternatives which had been in contrast with the proposed structure in Table 2, the basic structure with Adadelta training algorithm was the best. Hence, in rest of this section was distinguished as the unique alternative. As shown in Figure 2, the

range of accuracy variations across eight subjects according the proposed structure was considerably lower than its alternative.

In subject 1, the obtained variation ranges of the examined parameter (i.e. accuracy) for the proposed and basic structures were equal to 4.71% and 7.43%, respectively. These values showed that variations in the accuracy of the proposed structure were 2.72%

Figure 3: The results of application of the basic and the proposed structures on EPFL dataset for CNN based on True Positive Rate (TPR) across eight subjects

Figure 2: The results of application of the basic and the proposed structures on EPFL dataset for CNN based on accuracy across eight subjects
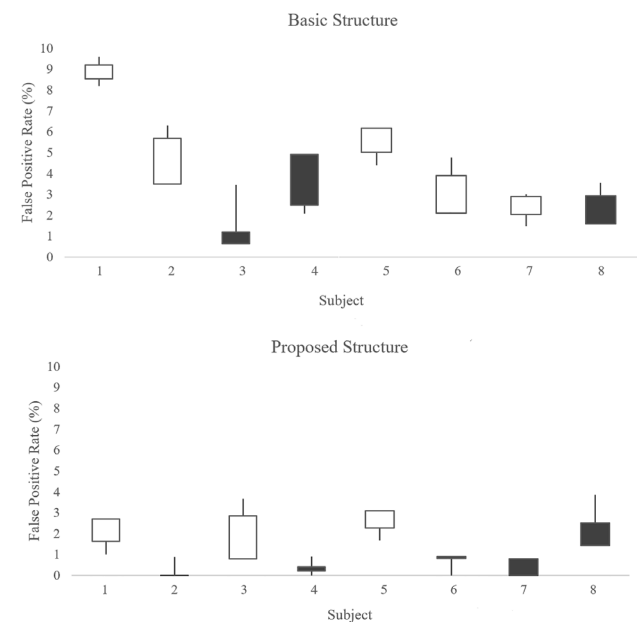
Figure 4: The results of application of the basic and proposed structures on EPFL dataset for CNN based on False Positive Rate (FPR) across eight subjects

more compact than the alternative structure during several runs. In subject 2, the proposed and alternative structures reached the range variations of 3.56% and 5.62% based on their accuracy. The obtained results showed that the proposed structure was 2.06% more stable than its alternative.

Similarly, the obtained ranges of accuracy using the proposed and alternative structures in subject 3 were equal to 2.51% and 3.23%, respectively. These results illustrated that the proposed structure had almost equal variations with the alternative structure in this subject. The variation ranges of accuracy in subject 4 were equal to 3.53% for the proposed structure and 4.31% for the alternative structure, which are somewhat similar to those of the previous subject.

In subject 5, the variation ranges for the proposed and alternative structures were 4.99% and 8.1%, respectively, showing considerable stability in the proposed structure compared to the basic structure. The obtained variation ranges in subject 6 were equal to 19.93% for the proposed structure and 9.8% for the alternative structure, again confirming the above fact.

In a similar manner, the variation ranges of the accuracy for the proposed and alternative structures in subject 7 were 3.17% and 4.81%, respectively; in subject 8 they were equal to 4.3% and 2.9%, respectively. In Figures 3 and 4, the stability of the proposed and basic structures was explored from another point of view. In these Figures, the range of variations in TPR and FPR obtained across all subjects was investigated.

In subject 1, the TPR variation range was equal to 8.8% for the proposed structure, whereas the variation range for its alternative was 14.53 %. However, the distance variation ranges of FPR showed that the proposed structure was almost as stable as the basic structure, as shown in Figure 4.

In subject 2, the obtained variation ranges of TPR for the proposed and alternative structures were equal to 7.11% and 10.89%, respectively. These values were 0.87% and 2.81% for their FPRs which revealed that based on both TPR and FPR the proposed structure was more stable than the basic structure. A glance on subject 3 showed that the variation ranges of TPRs in the proposed and alternative structures were 4.31% and 6.53%. On the other hand, the variation ranges of FPRs for the proposed structure were almost equal to the alternative structure. Likewise, the variation ranges of TPRs in subject 4 were equal to 6.85% for the proposed structure and 7.36% for the alternative structure. In addition, the variation ranges of FPR in this subject illustrated that the proposed structure, as compared to the alternative structure, was 1.94%

more stable.

In subject 5, the variation ranges of TPR for the proposed and alternative structures were 9% and 16.1%, respectively. Moreover, the variation ranges of FPR indicated that the proposed structure was as stable as the alternative one. Therefore, the more excellent stability of the proposed structure in TPR had not caused instability in FPR.

Similarly, the obtained variation ranges of TPR by subject 6 were equal to 3.57% for the proposed structure and 17.85% for the alternative structure, whereas the FPR of the proposed structure was 1.84% more stable than the alternative one.

The variation ranges of TPR in subject 7 were 6.82% for the proposed structure and 8.68% for the alternative structure. Furthermore, in subject 8 these values were equal to 6.24% for the proposed structure and 8.99% for the alternative structure. Also, the variation ranges of FPR for the proposed structure in subjects 7 was almost equal to that of the alternative structure. Similarly, in subject 8, the variation ranges of FPR for the proposed structure was almost equal to that of the alternative structure. Therefore, the more considerable stability of the TPR obtained by the proposed structure in these subjects had not caused instability in FPR.

The first four subjects were disabled and the next four were healthy persons. As displayed in Table 2, by applying the proposed algorithm some healthy subjects (for example subjects 6 and 7 with 98.97% and 98.77% accuracies, respectively) obtained better results than disabled ones. In the same manner, application of the proposed algorithm led to better results for some disabled persons (for example in subjects 2 and 4 with 97.45% and 98.57% classifications accuracy, respectively). Therefore, it may be concluded that the results are not relevant to the health condition of subjects.

Discussion

The BCI systems are composed of three main parts including data acquisition, preprocessing and classification. We developed the proposed method to improve the performance of the third part, based on sparse representation-based classification that extracted features which had less dependency on artifacts and noise. This idea led to higher detection rate in P300 signal relying on the so-called more clear features of the P300 signal.

The literature review showed that the proposed method had better performance than previous schemes. This is consistent with the results of some other studies (27), (28),(29). Two major disadvantages

of previous models are choosing appropriate features and tuning hyperparameters of the model (i.e. preparing sufficient generalization performance). The linear methods utilize appropriate lines as borders between classes to solve the problem; therefore, they are not robust against even little changes in data (27). On the other hand, neural networks are able to solve the problem by utilizing a set of hyperplanes. Unfortunately, the classic neural networks (for example, Multilayer Perceptrons) may not guarantee that their stopping minima is optima; therefore, they get stuck in a local minimum. One option for mitigating this phenomenon is to train these neural networks several times and each time by using different random starting position. Finally, the neural network that results 9in the best RMS error is selected (28). The number of random training iterations is one of the challenging issues in the above methods. Although some methods such as Random Training Iterations (RTI) might be used to set the number of iterations, this technique dramatically increases the total training time. Another limitation of the above algorithm is setting the number of hidden neurons. Selecting too low values for this parameter may result in underfitting for the neural network, while setting this value too high may result in overfitting (29).

The proper features and detection method affect the accuracy of the BCI reaction. Overall, the proposed method was very well accepted and gained high superiority against all the alternatives. For example, the accuracy of the proposed method was in the range of 6- 11%] better than those which had been obtained by well-known methods such as Linear Discriminant Analysis (LDA), Support Vector Machine (SVM) and classic Neural Networks.

Limitations

One of the limitations of this study was the nature and properties of the EEG signals. This signal has poor spatial resolution and high sensitivity to a particular set of post-synaptic potentials, those generated in superficial layers of the cortex, on the crests of gyri directly abutting the skull and radial to the skull. Dendrites, which are deeper in the cortex, have far less contribution to the EEG signal.

Furthermore, in EEG recordings the axonal action potentials are not directly captured. An action potential may be accurately represented as a current quadrupole, meaning that the resulting field decreases more rapidly than the ones produced by the current dipole of post-synaptic potentials. These facts lead to low SNR of the recorded signals which is the most common problem to detect the P300 signal in BCI

systems. Another cumbersome problem is selecting the reference electrode. In P300-based BCI, the most common referenced electrode is the electrode which is located on mastoid. Positioning of the electrode in this situation enables it to record a reflection of other brain activities in the rest of electrodes. Therefore, the recorded signal by this electrode may be utilized as a reference for reducing artifacts.

Another important issue is the method of application of the data in training and test of the deep neural structure. The four-fold cross-validation strategy was used in this research to evaluate the average examined parameters based on the fact that the data were recorded in four sessions. This process may be generalized to more folds if data gathering scenario contains more sessions. Finally, the dynamic range of the recorded signal may be seriously problematic in the neural network training and testing processes. We made an attempt to overcome this problem by using the normalization technique.

Advices

For the use of EEG for BCI applications, it is necessary to capture signals in a special scale and scheduling. In this study, the subjects were selected equally from the healthy and disabled persons. Furthermore, during the capture, a resting time was proposed to make them more centralized. Another important tip is related to different efficiencies for different recording channels. Actually, the recordings of electrodes are seriously different because some regions of the brain make the P300 signal more suitable than others. Therefore, it may be concluded that rejecting those electrodes which carry weaker (i.e. less informative) P300 signals is so effective in improving the efficiency of BCI application. On this basis, it is recommended that the process of selecting the best (i.e. optimum) electrodes should be added to the P300 detection process. It seems that such a strategy may improve the accuracy of the system parallel with the reduction of the number of channels which lead to faster process. Development of such a strategy is recommended to be investigated in future. Last but not the least, initial investigations on bitrate parameter revealed that this parameter showed a meaningful difference between the normal and disabled persons. In future works, we suggest that healthy and unhealthy subjects should be distinguished based on the measured bitrates which are obtained from their EEG signals.

Conclusion

In this study, a novel structure was introduced

to increase the ability of deep neural networks in distinguishing P300 and non-P300 signals. The proposed structure consists of two connected substructures; the first one was responsible for predicting the expected signal among signals combined with artifact and the second substructure got the predicted P300 signal to tag it as P300 or non-P300 signal.

To evaluate the proposed structure, we compared it with the basic structure which had been trained by Adadelta, Adam and RMSprop based on their classification accuracy. The obtained results illustrated that the proposed structure was achieved to the accuracy maximally10.46% better than the basic structure.

On the other hand, it was investigated that the performance of the proposed scheme is more robust than the basic structure. The classification accuracies which were obtained with the proposed structure based on different subjects showed a maximum variation of 6.68%, while that value which had been obtained by the basic structure was 9.8%. Based on the above analyses, it may be concluded that the proposed structure has a considerable potential to be used as P300 detection model in BCI applications.

Conflict of Interest: None declared.

References

1. Espinosa R. Increased Signal to Noise Ratio in P300 Potentials by the Method of Coherent Self-Averaging in BCI Systems. *International Scholarly and Scientific Research & Innovation*. 2013;7(11):386-90.

2. Cecotti H, Graser A. Convolutional neural networks for P300 detection with application to brain-computer interfaces. *IEEE Trans Pattern Anal Mach Intell*. 2011;33(3):433-45. doi: 10.1109/TPAMI.2010.125.

3. da Silva-Sauer L, Valero-Aguayo L, de la Torre-Luque A, Ron-Angevin R, Varona-Moya S. Concentration on performance with P300-based BCI systems: a matter of interface features. *Appl Ergon*. 2016;52:325-32. doi: 10.1016/j.apergo.2015.08.002.

4. Mubeen MA, Knuth KH. Evidence-Based Filters for Signal Detection: Application to Evoked Brain Responses. *arXiv preprint arXiv:11071257*. 2011.

5. Alvarado-Gonzalez M, Garduno E, Bribiesca E, Yanez-Suarez O, Medina-Banuelos V. P300 Detection Based on EEG Shape Features. *Comput Math Methods Med*. 2016;2016:2029791. doi: 10.1155/2016/2029791.

6. Donchin E, Spencer KM, Wijesinghe R. The mental prosthesis: assessing the speed of a P300-based brain-computer interface. *IEEE Trans Rehabil Eng*. 2000;8(2):174-9.doi: 10.1109/86.847808.

7. Vareka L, Mautner P, editors. Using the Windowed means paradigm for single trial P300 detection. 2015 38th International Conference on Telecommunications and Signal Processing (TSP); 2015: IEEE.doi: 10.1109/tsp.2015.7296414.

8. Hutagalung SS, Turnip A, Munandar A, editors. P300 detection based on extraction and classification in online BCI. 2013 3rd International Conference on Instrumentation Control and Automation (ICA); 2013: IEEE.doi: 10.1109/ica.2013.6734042.

9. Sobhani A, editor P300 classification using deep belief nets. European Symposium on Artificial Neural Networks (ESANN); 2014.

10. Magee R, Givigi S, editors. A genetic algorithm for single-trial P300 detection with a low-cost EEG headset. 2015 Annual IEEE Systems Conference (SysCon) Proceedings; 2015. doi: 10.1109/syscon.2015.7116757.

11. Goodfellow I, Bengio Y, Courville A. Deep learning. Cambridge: MIT press; Vol. 1. 2016.

12. Kawaguchi K, editor Deep learning without poor local minima. Adv Neural Inf Process Syst; 2016. (pp. 586-594).

13. Zhang J, Yan C, Gong X, editors. Deep convolutional neural network for decoding motor imagery based brain computer interface. 2017 IEEE International Conference on Signal Processing, Communications and Computing (ICSPCC); 2017: IEEE. [1] (pp. 1-5).doi: 10.1109/icspcc.2017.8242581.

14. Maddula R, Stivers J, Mousavi M, Ravindran S, de Sa V, editors. Deep recurrent convolutional neural networks for classifying P300 BCI signals. Proceedings of the Graz BCI Conference; 2017.

15. Ge R, Huang F, Jin C, Yuan Y, editors. Escaping from saddle points—online stochastic gradient for tensor decomposition. Conference on Learning Theory; 2015. (pp. 797-842).

16. Geraci JR, Kapoor P. A method of limiting performance loss of CNNs in noisy environments. *arXiv preprint arXiv:170200932*. 2017.

17. Hoffmann U, Vesin JM, Ebrahimi T, Diserens K. An efficient P300-based brain-computer interface for disabled subjects. *J Neurosci Methods*. 2008;167(1):115-25. doi: 10.1016/j.jneumeth.2007.03.005.

18. LeCun Y [Internet]. LeNet-5, convolutional

neural networks. c2015. Available from: URL: http://yann lecun com/exdb/lenet

19. Zhang W, editor Shift-invariant pattern recognition neural network and its optical architecture/Wei Zhang. Proceedings of annual conference of the Japan Society of Applied Physics–1988.

20. Zhang W, Itoh K, Tanida J, Ichioka Y. Parallel distributed processing model with local space-invariant interconnections and its optical architecture. *Applied optics.* 1990;29(32):4790-7. doi: 10.1364/AO.29.004790.

21. Matsugu M, Mori K, Mitari Y, Kaneda Y. Subject independent facial expression recognition with robust face detection using a convolutional neural network. *Neural networks : the official journal of the International Neural Network Society.* 2003;16(5-6):555-9. doi: 10.1016/S0893-6080(03)00115-1.

22. Karpathy A. Cs231n convolutional neural networks for visual recognition. *Neural networks.* 2016;1.

23. Vu TH, Nguyen L, Le C, Monga V, editors. Tensor sparsity for classifying low-frequency ultra-wideband (UWB) SAR imagery. 2017 IEEE Radar Conference (RadarConf); 2017: IEEE. (pp. 0557-0562).doi: 10.1109/radar.2017.7944265.

24. Nguyen LH, Kappra KA, Wong DC, Kapoor R, Sichina J, editors. Mine field detection algorithm utilizing data from an ultrawideband wide-area surveillance radar. Detection and Remediation Technologies for Mines and Minelike Targets III; 1998: International Society for Optics and Photonics. (Vol. 3392, pp. 627-644).

25. Stutz D. Understanding convolutional neural networks. InSeminar Report, Fakultät für Mathematik, Informatik und Naturwissenschaften Lehr-und Forschungsgebiet Informatik VIII Computer Vision. 2014.

26. Ruder S. An overview of gradient descent optimization algorithms. *arXiv preprint arXiv:160904747.* 2016.

27. Kundu S, Ari S, editors. P300 Detection Using Ensemble of SVM for Brain-Computer Interface Application. 2018 9th International Conference on Computing, Communication and Networking Technologies (ICCCNT); 2018: IEEE.doi: 10.1109/icccnt.2018.8493903.

28. Manyakov NV, Chumerin N, Combaz A, Van Hulle MM. Comparison of classification methods for P300 brain-computer interface on disabled subjects. *Comput Intell Neurosci.* 2011;2011:519868. doi: 10.1155/2011/51986.

29. Cecotti H, Gräser A, editors. Neural network pruning for feature selection-Application to a P300 Brain-Computer Interface. ESANN; 2009.